

# Sliding bifurcations and non-determinism in systems with switching

Mike R Jeffrey\*

\* Dept. of Engineering Mathematics, University of Bristol, Queen's  
Building, Bristol BS8 1TR, UK. email: mike.jeffrey@bristol.ac.uk

---

**Abstract:** Dynamical events associated with loss of determinacy in piecewise-smooth dynamical systems are reviewed. The causes of non-determinacy are discussed, and the conditions for their occurrence in general systems are derived. These events can be characterized in terms of recently classified catastrophic sliding bifurcations and a non-deterministic form of chaos, which are shown to provide generic scenarios for non-determinacy to affect stable dynamical behaviour. The particular conditions for these are derived in a canonical (Lur'e) model of switched feedback control, and explicit examples are given in two and three dimensions.

*Keywords:* Switching surfaces, Determinism, Control models

---

## 1. INTRODUCTION

A variety of dynamical phenomena have come to light in recent years associated with *sliding modes* in systems of piecewise-smooth ordinary differential equations. Such systems contain hypersurfaces where the differential equations are discontinuous, called *switching manifolds*. Sliding modes are solutions constrained to evolve on the hypersurface. Early interest in discontinuity-induced bifurcations in such systems has naturally focused on regions of a switching manifold that are attractive, and where sliding occurs. The result is that periodic orbits can acquire segments of sliding by so-called *sliding bifurcations* (di Bernardo et al., 2003, 2008). The scenario of sliding in a region where solutions are repelled from the switching manifold (sometimes called *escaping*), appears at first to be of less interest dynamically, because one expects solutions to evolve away from the discontinuity. In the present paper we discuss the dynamical consequences of generic scenarios where solutions evolve *into* repelling regions of sliding, showing that non-determinacy enters into the dynamics. This results in novel forms of bifurcations and chaos peculiar to piecewise-smooth systems. We derive the conditions for each in a model of switched feedback control.

Such repelling regions of sliding have been shown to give rise to *catastrophic* forms of sliding bifurcations (Jeffrey et al., 2010), whose effect on periodic orbits is instantaneous destruction, without any incipient change in period or amplitude (in contrast to smooth systems, see e.g. Kuznetsov (1998)). The meeting between attracting and repelling regions of sliding has also been shown to produce repetitive yet unpredictable dynamics, constituting a non-deterministic form of chaos Colombo and Jeffrey (2011). The conditions for all these behaviours have been derived across a number of papers by Colombo et al. (2010); Colombo and Jeffrey (2011); Jeffrey and Hogan (2011), but are presented here in a general form applicable to any piecewise-smooth (Filippov) system, and then applied to a typical model of switched feedback control.

We present examples in linear systems to demonstrate the simplicity of these phenomena, but all of the results derived apply to general systems, irrespective of linearity.

Consider the dynamical solutions possible when a system of ordinary differential equations

$$\dot{x} = \begin{cases} f^+(x) & \text{if } \sigma(x) > 0, \\ f^-(x) & \text{if } \sigma(x) < 0, \end{cases} \quad (1)$$

are satisfied by a state  $x \in \mathbb{R}^n$ , where  $f^\pm : \mathbb{R}^n \mapsto \mathbb{R}^n$  are smooth functions. This has a switching manifold given by

$$\Sigma := \{x \in \mathbb{R}^n : \sigma(x) = 0\}, \quad (2)$$

where the switching function  $\sigma : \mathbb{R}^n \mapsto \mathbb{R}$  is smooth everywhere, and  $\partial_x \sigma \neq 0$ . Solutions can then be constructed in such a way that orbits  $x(t) : \mathbb{R} \mapsto \mathbb{R}^n$  are continuous, but are non-differentiable where they meet  $\Sigma$ .

In section 2, the standard method for solving (1) is summarized, in a manner that facilitates our study of the appearance of non-determinacy in section 3. We review the resulting bifurcations and chaos, bringing new notions in these areas together in a coherent framework. These are used in section 4 to derive conditions for non-deterministic phenomena in switched feedback control systems and piecewise-linear flows, illustrated with examples.

## 2. SLIDING AND CROSSING

To study (1), we will frequently require the rate of change of  $\sigma$  along an orbit,

$$\frac{d}{dt}\sigma(x(t)) = \begin{cases} \mathcal{L}_{f^+}\sigma(x) & \text{if } \sigma(x) > 0, \\ \mathcal{L}_{f^-}\sigma(x) & \text{if } \sigma(x) < 0, \end{cases} \quad (3)$$

where  $\mathcal{L}_f = f \cdot \partial_x$  is the Lie derivative along the vector field  $f$ , (and the second derivative is denoted  $\mathcal{L}_f^2 = (\mathcal{L}_f)^2$ ).

If the flow encounters a point on  $\Sigma$  where  $f^+$  and  $f^-$  have the same directions normal to  $\Sigma$ , we concatenate solutions from either side of  $\Sigma$ , forming orbits  $x(t)$  which cross the switching manifold over a region labelled  $\Sigma_c$ , illustrated in Fig. 1(i). If the flow encounters a point where  $f^+$  and

$f^-$  both point towards  $\Sigma$ , then the state at later times is evidently constrained to  $\Sigma$  over some region labelled  $\Sigma^s$ , which we call *stable sliding*, shown in Fig. 1(ii). Solutions can then be found by forming a differential inclusion,

$$\dot{x} \in \lambda f^+ + (1 - \lambda) f^-, \quad \lambda \in [0, 1] \quad (4)$$

such that  $\lambda = 1$  if  $\sigma > 0$  and  $\lambda = 0$  if  $\sigma < 0$ . In practice, we need only add to (1) the *sliding vector field*  $f^{sl}$ , with

$$\dot{x} = f^{sl} \quad \text{if } \sigma = 0, \quad (5)$$

where

$$f^{sl} = \lambda f^+ + (1 - \lambda) f^-, \quad \lambda = \frac{\mathcal{L}_{f^-} \sigma}{(\mathcal{L}_{f^-} - \mathcal{L}_{f^+}) \sigma}. \quad (6)$$

Originally due to Filippov (1988), this convention corresponds algebraically, at least, to applying the equivalent control  $\beta = 2\lambda - 1$  of Utkin (1977). Orbits are constructed by concatenating solutions of the subsystems  $\dot{x} = f^+$ ,  $\dot{x} = f^-$ , and  $\dot{x} = f^{sl}$ , while preserving the direction of time. The evolution is then well-determined in forward time, although any point  $x \in \Sigma^s$  may have different possible histories in either  $\sigma > 0$ ,  $\sigma < 0$ , or  $\Sigma^s$ .

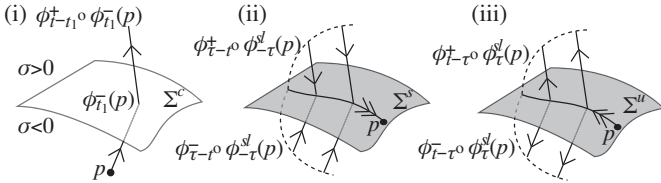


Fig. 1. Dynamics at a switching manifold. The flow through a point  $p$  is shown, formed by concatenating segments of flow  $\phi_t^+$  in  $\sigma > 0$ ,  $\phi_t^-$  in  $\sigma < 0$ , and  $\phi_t^{sl}$  on  $\sigma = 0$ . (i) Crossing the manifold; (ii) stable sliding; (iii) unstable sliding. In (ii) and (iii) orbits are parameterized by their sliding time  $\tau \in [0, t]$ . Throughout this paper, shaded regions and double arrows denote sliding.

Stable sliding is a desirable behaviour for controlling a system onto a state  $x$  that satisfies  $\sigma(x) = 0$ . A less often considered dynamical scenario arises where  $f^+$  and  $f^-$  both point away from  $\Sigma$ , labelled  $\Sigma^u$ . Similar to stable sliding, orbits are formed by concatenating solutions of the three subsystems  $\dot{x} = f^+$ ,  $\dot{x} = f^-$ , and  $\dot{x} = f^{sl}$ . In  $\Sigma^u$ , however, solutions of (4) are not uniquely determined in forward time, as every point  $x \in \Sigma^u$  has orbits not only remaining in  $\Sigma^u$ , but also escaping it into  $\sigma \neq 0$ . We call this *unstable sliding*, shown in Fig. 1(iii). Bringing these together, the three regions  $\Sigma^{c,s,u}$  are defined by

$$\Sigma^c = \{x \in \Sigma : (\mathcal{L}_{f^+} \sigma)(\mathcal{L}_{f^-} \sigma) > 0\}, \quad (7a)$$

$$\Sigma^s = \{x \in \Sigma : \mathcal{L}_{f^+} \sigma < 0 < \mathcal{L}_{f^-} \sigma\}, \quad (7b)$$

$$\Sigma^u = \{x \in \Sigma : \mathcal{L}_{f^-} \sigma < 0 < \mathcal{L}_{f^+} \sigma\}. \quad (7c)$$

### 3. ROUTES TO NON-DETERMINISM

The conditions (7b) and (7c) for sliding guarantee that (6) is well-defined in the sliding regions. Points where  $\mathcal{L}_{f^-} \sigma = 0$  (when  $\lambda = 0$ ) or  $\mathcal{L}_{f^+} \sigma = 0$  (when  $\lambda = 1$ ) form the boundaries of regions of sliding. These conditions mean that non-sliding orbits meet  $\Sigma$  with zero normal velocity; such orbits are said to *graze* the switching manifold. The boundaries are the only places where orbits of (1) can leave  $\Sigma^s$  or enter  $\Sigma^u$ , the latter of which we discuss below.

#### 3.1 Boundaries of unstable sliding: the grazing explosion

The simplest type of boundaries are *folds* (Filippov, 1988). Their definition states that, if  $\mathcal{L}_{f^i} \sigma$  vanishes at  $\sigma = 0$ , then  $\mathcal{L}_{f^i}^2 \sigma$  is non-vanishing, with  $i$  denoting  $+$  or  $-$ . Because an unstable sliding region is repelling with respect to the surrounding flow (recall Fig. 1(iii)), the only place that an orbit can enter  $\Sigma^u$  is at its boundary, and only if  $f^{sl}$  points inwards from the boundary. From (6), this requires that the flow curves away from  $\Sigma$ , which we describe as a *visible fold*. More precisely, a visible fold at the boundary of unstable sliding satisfies either:

$$\mathcal{L}_{f^+} \sigma = 0 \text{ and } \mathcal{L}_{f^+}^2 \sigma > 0, \quad \mathcal{L}_{f^-} \sigma < 0, \quad (8)$$

for grazing from above  $\Sigma$ , which is shown in Fig. 2, or

$$\mathcal{L}_{f^-} \sigma = 0, \text{ and } \mathcal{L}_{f^-}^2 \sigma < 0, \quad \mathcal{L}_{f^+} \sigma > 0, \quad (9)$$

for grazing from below  $\Sigma$ .

The dynamics at the boundary is as follows. Let  $\phi_t^i(p)$  denote the orbit of a point  $p$  after a time  $t$  evolving through  $f^i$ , where  $i$  is either  $+$ ,  $-$ , or  $sl$ . Let  $p$  be such that the orbit grazes  $\Sigma$  at time  $t = t_1$  as shown in Fig. 2(i). Then the orbit of  $p$  is unique for  $t < t_1$ , but thereafter the evolution is set-valued. The state  $x$  at a time  $t > t_1$  is given by

$$x \in \{x_\tau(t) = \phi_{t-t_1-\tau}^\pm \circ \phi_\tau^{sl} \circ \phi_{t_1}^+(p) : \tau \in [0, t-t_1]\},$$

where the solution slides after grazing for a time  $\tau \in [0, t-t_1]$ , then leaves  $\Sigma$ , following the flow of either  $f^+$  or  $f^-$ .

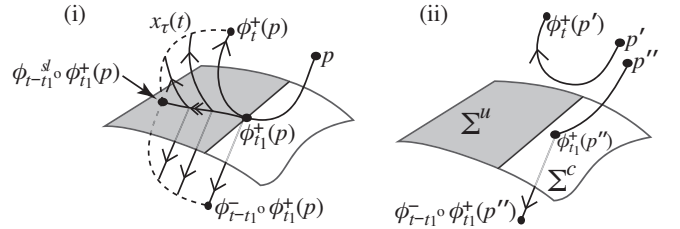


Fig. 2. Non-determinacy at a sliding boundary: the *grazing explosion*. In (i), the flow  $\phi^+$  of  $f^+$  from a point  $p$  grazes  $\Sigma$  at time  $t = t_1$ , after which the flow is a family of orbits  $x_\tau(t) = \phi_{t-t_1-\tau}^\pm \circ \phi_\tau^{sl} \circ \phi_{t_1}^+(p)$ , parameterized by the sliding time  $\tau \in [0, t-t_1]$ . (ii) shows the two kinds of orbit obtained by small perturbations of  $p$ , to  $p'$  or  $p''$ . The sliding region (shaded) is unstable.

Clearly the scenario in Fig. 2(i) is not structurally stable, as it requires  $\mathcal{L}_{f^+} \sigma(\phi_{t_1}^+(p)) = 0$  at a point where  $\sigma(\phi_{t_1}^+(p)) = 0$ . The explosion of possible states at the boundary is therefore a codimension one event, typically observed under variation of a parameter, whereby the orbit from a point  $p$  switches between the two types shown in Fig. 2(ii) and is instantaneously set-valued (the explosion) when grazing occurs. This transition was classified by Jeffrey and Hogan (2011) as a catastrophic form of sliding bifurcation, without focusing on the explosion itself.

This is the simplest way in which non-determinacy appears at a boundary. It has been shown to explain the sudden onset of self-sustaining thermal oscillations in a superconducting sensor device (Jeffrey et al., 2010). In that system, temperature control of a superconducting stripline resonator allows sensitive control of resistance. The switching manifold is a temperature threshold between the resonator's normal and superconducting states,

and controllability is lost when a grazing explosion creates an attractor in the form of large thermal oscillations.

The following example shows a simple grazing explosion.

**Example.** Let  $\sigma(x) = (x_2 + 1 + \mu)(c - x_2)$  where  $\mu \in \mathbb{R}$  and  $c = e^{-\pi/\sqrt{3}} \approx 0.16$ , with vector fields

$$f^+ = \begin{pmatrix} -x_2 \\ x_1 + x_2 + 1 \end{pmatrix}, \quad f^- = \begin{pmatrix} 0 \\ -1 \end{pmatrix}. \quad (10)$$

A grazing explosion is observed as  $\mu$  changes sign, with a unique periodic orbit for  $\mu > 0$ , an explosion of periodic orbits at  $\mu = 0$ , and the sudden disappearance of periodic orbits when  $\mu < 0$ .

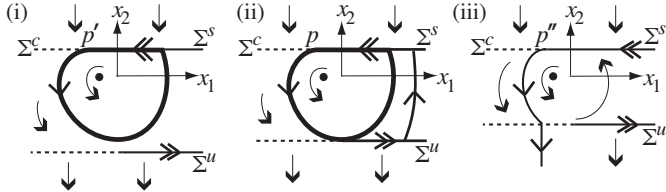


Fig. 3. Example of a grazing explosion in (10). Showing: (i)  $\mu = 0.01$ , a stable periodic orbit, (ii)  $\mu = 0$ , the orbit grazes, and infinitely many periodic orbits pass through  $\Sigma^u$  and  $\Sigma^s$ ; (iii)  $\mu = -0.01$ , no periodic orbits exist. The points  $p, p', p''$ , correspond to those in Fig. 2.

### 3.2 Two-fold at a boundary: the canard explosions

Grazing can occur simultaneously on both sides of  $\Sigma$ . Moreover, this generically occurs in systems of three or more dimensions when a pair of folds cross transversally. Such a point is called a *two-fold* singularity, and satisfies

$$\mathcal{L}_{f^+}\sigma = 0 \neq \mathcal{L}_{f^+}^2\sigma, \quad (11a)$$

$$\mathcal{L}_{f^-}\sigma = 0 \neq \mathcal{L}_{f^-}^2\sigma, \quad (11b)$$

$$\det[\partial_x\sigma, \partial_x(\mathcal{L}_{f^+}\sigma), \partial_x(\mathcal{L}_{f^-}\sigma)] \neq 0. \quad (11c)$$

At a two-fold, the sliding vector field  $f^{sl}$  is no longer well defined by (6) because of the double zero in (11a)-(11b). We must therefore return to the set-valued equations (4), and if trajectories in the stable and unstable sliding regions meet at a two-fold we can concatenate them. This forms an orbit that crosses the two-fold either from stable to unstable sliding, which we refer to as a *canard*, or conversely from unstable to stable sliding, referred to as a *faux canard*. The names are derived from corresponding orbits responsible for ‘‘canard explosions’’ in slow-fast systems (Benoît et al., 1981); this correspondence has been partly formalised by Desroches and Jeffrey (2011).

Fig. 4 illustrates two possible scenarios resulting when the orbit  $\phi_t^{sl}(p)$  of a point  $p$  in the stable sliding region hits a two-fold at time  $t = t_1$ . Depending on the form of  $f^{sl}$  from (6), there may exist zero, one, or many sliding orbits through the two-fold, the latter two cases being shown in Figs. 4 (i)-(ii) respectively. The state at a time  $t > t_1$  is a family of orbits which slide for a time  $\tau \in [0, t - t_1]$ , then follow  $f^+$  or  $f^-$  until time  $t$ . These states are given by

$$x \in \{ x_\tau(t) = \phi_{t-t_1-\tau}^\pm \circ \phi_\tau^{sl} \circ \phi_{t_1}^{sl}(p) : \tau \in [0, t - t_1] \},$$

Similarly to the grazing explosion in the previous section, the scenario shown in Fig. 4(i) is not structurally stable, but the scenario in (ii) is. The orbit through  $p$  satisfies

the conditions  $\mathcal{L}_{f^+}\sigma(\phi_{t_1}^{sl}(p)) = \mathcal{L}_{f^-}\sigma(\phi_{t_1}^{sl}(p)) = 0$ , but to determine the codimension of this event requires analysing the topology of the sliding vector field. Below we summarize the conditions under which such canards arise.

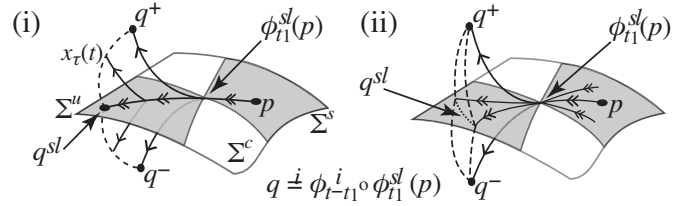


Fig. 4. Non-determinacy at a two-fold: the *canard explosions*, consisting of flow segments  $\phi_t^\pm$  and sliding segments  $\phi_\tau^{sl}$ , parameterized by the duration of sliding  $\tau$  after the flow crosses the two-fold at  $t = t_1$ . The flow becomes non-deterministic as it passes from stable to unstable sliding. The unstable sliding trajectory  $\phi_\tau^{sl} \circ \phi_{t_1}^{sl}(p)$  is single-valued in (i) and set-valued in (ii).

### 3.3 Conditions for existence of canards

The sliding vector field local to a two-fold was already well studied by Filippov (1988). Recently, Jeffrey and Hogan (2011) have shown, in arbitrary dimensions, that a one-parameter sliding bifurcation at a two-fold can take any of the forms shown in Fig. 5.

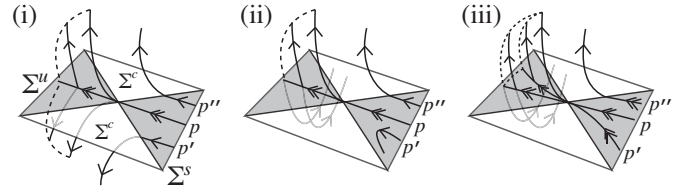


Fig. 5. Classification of canard explosions: (i) visible canard, (ii) simple canard, (iii) robust canard. In (i) the folds are both visible, in (ii) one is visible and the other invisible.

The point  $p$  produces a canard explosion of the forms considered in Fig. 4. If a perturbation shifts  $p$  by a small amount to  $p'$  or  $p''$ , the phase portrait changes discontinuously. If  $p$  lies on, for example, a periodic orbit, this transition constitutes a catastrophic form of sliding bifurcation, in which the periodic orbit can persist only on one side of the bifurcation (Jeffrey and Hogan, 2011).

The local conditions for these different forms of canards to occur, when an orbit intersects a two-fold, were derived by Jeffrey and Hogan (2011) in terms of certain normal forms. Below these are recast into conditions for a general vector field. We have first to define two quantities characterising the relative directions of the vector fields  $f^\pm$ :

$$w^+ = \frac{\mathcal{L}_{f^+}\mathcal{L}_{f^-}\sigma}{\sqrt{-\mathcal{L}_{f^+}^2\sigma\mathcal{L}_{f^-}^2\sigma}}, \quad w^- = \frac{-\mathcal{L}_{f^-}\mathcal{L}_{f^+}\sigma}{\sqrt{-\mathcal{L}_{f^+}^2\sigma\mathcal{L}_{f^-}^2\sigma}}, \quad (12)$$

evaluated at the two-fold, given by (11). The denominators of  $w^\pm$  (12) are nonzero by the inequalities in (11a)-(11b).

For the *visible canard* in Fig. 5(i) to occur, the following conditions are necessary and sufficient:

$$\mathcal{L}_{f^+}\sigma > 0 > \mathcal{L}_{f^-}\sigma \quad \text{with} \quad (13a)$$

$$w^+ \leq 0 \text{ and/or } w^- \leq 0 \text{ and/or } w^+w^- < 1, \quad (13b)$$

evaluated at the two-fold. Condition (13a) means the flow curves away from  $\Sigma$  at both folds (called *visible* folds), and (13b) implies the existence of a canard. A visible canard explosion has codimension one. For the simple canard in Fig. 5(ii), necessary and sufficient conditions are

$$(\mathcal{L}_{f^+}^2\sigma)(\mathcal{L}_{f^-}^2\sigma) > 0 \quad \text{with} \quad (14a)$$

$$\tilde{w}^+, \tilde{w}^- > 0 \quad \text{and} \quad \tilde{w}^+ \tilde{w}^- > 1, \quad (14b)$$

where  $w^\pm$  are imaginary, so we introduce  $w^\pm = \mp i\tilde{w}^\pm$  where  $i = \sqrt{-1}$ . The *simple canard* explosion also has codimension one. The remaining case, however, contains a family of canards: the orbit through  $p'$  in Fig. 5(iii) persists under small perturbation, and it is only for large perturbation through to  $p''$  that the canard is lost. This is a *robust canard*, with necessary and sufficient conditions

$$(\mathcal{L}_{f^+}^2\sigma)(\mathcal{L}_{f^-}^2\sigma) > 0 \quad \text{with} \quad (15a)$$

$$\tilde{w}^+ \tilde{w}^- < 1 < (\tilde{w}^+ + \tilde{w}^-)/2, \quad \text{and} \quad (15b)$$

$$(\tilde{w}^+ - \tilde{w}^-)\mathcal{L}_{f^\pm}^2\sigma > 0. \quad (15c)$$

Conditions (14a) and (15a) mean the flow curves away from  $\Sigma$  at one fold (a *visible* fold) and towards  $\Sigma$  at the other (called an *invisible* fold). (14b) gives existence of a single canard, and (15b)-(15c) give existence of a family of canards (as shown by Colombo and Jeffrey (2011)).

**Remark.** If (13b) is violated in (13), or if  $\tilde{w}^+ \tilde{w}^- > 1$  in (14), we obtain a “faux canard”, an orbit passing from unstable to stable sliding. Similarly if (15c) is violated in (15) we obtain a family of faux canards. If none of the sets of conditions above hold, then no canards exist.

**Example.** Let  $x = (x_1, x_2, x_3)^\top$ ,  $\sigma(x) = x_2$ , and

$$f^+ = \begin{pmatrix} x_2 - 1 \\ \frac{1}{10}x_2 - x_1 \\ \frac{1}{10}(\mu - x_3) \end{pmatrix}, \quad f^- = \begin{pmatrix} -1 \\ x_1 - x_3 \\ 0 \end{pmatrix}, \quad (16)$$

for  $\mu \in \mathbb{R}$ . This system is sketched in Fig. 6, and shows a periodic orbit with a sliding segment being destroyed suddenly as  $\mu$  varies, when it forms a canard explosion through a visible two-fold at  $\mu = 0$ .

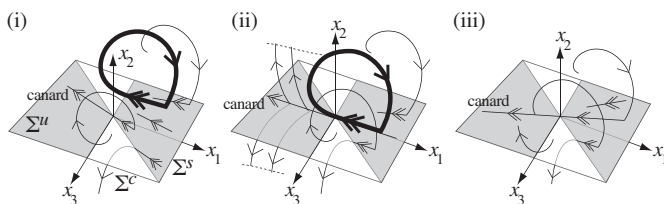


Fig. 6. A period orbit destroyed in a visible canard explosion. A pair of folds cross at the two-fold at the origin. (i) When  $\mu < 0$  a unique periodic orbit exists in the region  $x_2 \geq 0$ ; (ii) when  $\mu = 0$  this orbit lies on a canard; and (iii) when  $\mu > 0$  no periodic orbits exist.

### 3.4 Non-deterministic chaos

We have omitted from above the fourth and final case of canards at a two-fold, which occurs at a point where

$$\mathcal{L}_{f^+}^2\sigma < 0 < \mathcal{L}_{f^-}^2\sigma \quad \text{with} \quad (17a)$$

$$w^\pm < 0 \quad \text{and} \quad w^+ w^- > 1. \quad (17b)$$

(17a) means the flow curves towards  $\Sigma$  at both folds (which are therefore called *invisible* folds), and (17b) implies the

existence of canards (and faux canards otherwise). When these *invisible canards* occur, every orbit through the two-fold is a canard. This makes invisible canards robust to parameter variation, with particularly novel consequences.

A detailed study has only been made in three dimensions, by Colombo and Jeffrey (2011), who observe an interesting behaviour when  $w^+ w^- \approx 1$ . A bifurcation occurs at  $w^+ w^- = 1$ , in which a fixed point is born in the unstable sliding region, and a limit cycle is born passing through the crossing regions. In the case when the fixed point is stable and the cycle is unstable, the dynamics is illustrated in Fig. 7. A one-dimensional centre manifold can be found for  $f^{sl}$  such that sliding dynamics takes the form

$$\dot{u} = (w^+ w^- - 1)u + au^2 + \mathcal{O}(u^3), \quad a > 0. \quad (18)$$

A map can also be found describing the return of orbits to either of the crossing regions, in the form

$$\begin{pmatrix} \dot{u}_1 \\ \dot{u}_2 \end{pmatrix} = \begin{pmatrix} u_1 + \mathcal{O}(u_1^4, u_2^4) \\ bu_1 u_2 + cu_1^3 + du_1^2 u_2 + \mathcal{O}(u_1^4, u_2^4) \end{pmatrix}, \quad (19)$$

where  $c < 0$ . These conditions guarantee that all local

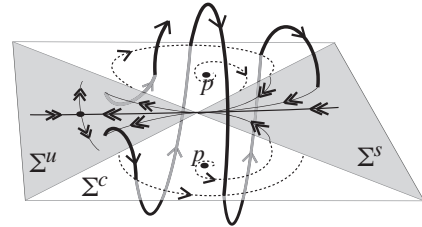


Fig. 7. A non-deterministic form of chaos. Orbits wind around an invisible two-fold. Their return map through the crossing regions  $\Sigma^c$  is shown by dotted paths spiraling out from  $p$ , which lies on an unstable periodic orbit of the 3D system. All orbits reach  $\Sigma^s$  in finite time, then pass through the two-fold along a canard. As in Fig. 4(ii), the state after crossing the two-fold is set-valued, but all solutions eventually return to the two-fold.

orbits will enter the two-fold along a canard, and moreover will visit the two-fold recurrently, but, recalling Fig. 4(ii), on each visit the orbit’s evolution becomes non-deterministic. Thus their amplitude of excursion and number of rotations around the folds is unpredictable, but they will always return to the two-fold in finite time. This recurrent but unpredictable behaviour has been described as a non-deterministic form of chaos, a precise definition being provided by Colombo and Jeffrey (2011).

## 4. CONDITIONS FOR FOLDS AND TWO-FOLDS IN SWITCHED FEEDBACK CONTROL

We now consider when the phenomena above can be found in a common practical scenario, namely switched feedback control. Following Colombo et al. (2010), we begin with the classical Lur’e problem with  $p$  outputs and  $m$  inputs, in which a state  $x \in \mathbb{R}^3$  evolves according to

$$\dot{x} = Ax + Bu, \quad (20a)$$

$$y = Cx, \quad (20b)$$

where  $u \in \mathbb{R}^m$ ,  $A \in \mathbb{R}^{3 \times 3}$ ,  $B \in \mathbb{R}^{3 \times m}$ ,  $y \in \mathbb{R}^p$ ,  $C \in \mathbb{R}^{p \times 3}$ . A feedback action is described by  $u = -\phi(y)$ , where  $\phi: \mathbb{R}^p \mapsto \mathbb{R}^m$  is a piecewise affine function of the form

$$\phi = \begin{cases} H^+ y + E^+ & \text{if } \sigma(y) > 0, \\ H^- y + E^- & \text{if } \sigma(y) < 0, \end{cases} \quad (21)$$

with  $H^\pm \in \mathbb{R}^{m \times p}$  and  $E^\pm \in \mathbb{R}^m$ . The switching function  $\sigma : \mathbb{R}^p \mapsto \mathbb{R}$  is given by  $\sigma(y) = Sy + s_0$ , where  $S \in \mathbb{R}^{1 \times p}$  and  $s_0 \in \mathbb{R}$ . Without loss of generality we let  $s_0 = 0$  and  $S \neq 0$ , giving a switching manifold  $\Sigma := \{x \in \mathbb{R}^3 : SCx = 0\}$ . This then takes the form (1), with vector fields

$$f^\pm = J^\pm x - BE^\pm, \quad (22)$$

where  $J^\pm = A - BH^\pm C$  are the Jacobian matrices of  $f^\pm$ .

To calculate whether folds exist and are non-degenerate we require the following quantities from section 3, found by straightforward calculation:

$$\sigma = SCx, \quad (23a)$$

$$\mathcal{L}_{f^i} \sigma = SCf^i, \quad (23b)$$

$$\mathcal{L}_{f^i}^2 \sigma = SCJ^i f^i, \quad (23c)$$

$$\mathcal{L}_{f^i} \mathcal{L}_{f^j} \sigma = SCJ^j f^i, \quad (23d)$$

where  $i, j$ , are either  $+$  or  $-$ . Recall that (23a) vanishes on the switching manifold, and that for a fold (23b) must vanish for one vector field but not for the other, while (23c) must not vanish by (8)-(9). For a two-fold, (23b) must vanish for both vector fields while (23c) must not vanish by (11). To establish whether two-folds are non-degenerate we also require, from (11c), that

$$\det(\dots) = \det(SCJ^+, SCJ^-, SC) \quad (24)$$

is non-vanishing, and to classify dynamics at a two-fold from (12) we need the quantities

$$w^\pm = \frac{\pm SCJ^\mp f^\pm}{\sqrt{-SCJ^+ f^+ - SCJ^- f^-}}. \quad (25)$$

#### 4.1 SISO and SIMO

In the case of a single input and single output (SISO), the quantities  $Cx$ ,  $CB$ ,  $S$  and  $H^\pm$  are all scalars. The determinant in (24) can then be re-arranged into

$$\det(\dots) = S^3 CB(H^+ - H^-) \det(CA, C, C), \quad (26)$$

which clearly vanishes since the last two terms inside the determinant are identical. This means a pair of folds can exist, and if  $CBE^\pm = 0$  they intersect, but do so non-transversally since (26) vanishes (Colombo et al. (2010)).

For a single input multiple output (SIMO), the quantity  $SCB$  is a scalar. The two fold conditions (11a)-(11b) give  $SCf^\pm = 0$ , implying by (22) that

$$SC(f^+ - f^-) = SCBQ = 0, \quad (27)$$

where  $Q = (H^+ - H^-)Cx + E^+ - E^-$  determines the size of the applied control. This implies that either  $SCB = 0$  or  $Q = 0$ . The determinant (24), which in terms of  $Q$  is simply  $SCB \det[SC\partial_x P, \partial_x Q, SC]$ , must not vanish, hence  $SCB \neq 0$ , and therefore  $Q = 0$ . This is a general proof of a result found for a specific example in Colombo et al. (2010), that continuity between  $f^+$  and  $f^-$  is achieved at generic two-folds in SIMO systems. Note, however, that the derivatives  $J^+$  and  $J^-$  are still non-equal. Nevertheless, when we substitute  $f^+ = f^-$  into (25) for  $J^+ \neq J^-$ , we find that  $w^+ w^- = 1$ , meaning SIMO systems are confined to lie on the boundary of the inequalities in the canard conditions (13)-(15).

#### 4.2 MIMO

Let us finally consider examples of the general case, of multiple input multiple output (MIMO) systems.

**Example.** In switched state feedback control, the full state is available for feedback, hence  $C$  is the  $3 \times 3$  identity matrix and  $y = x$ . The folds are solutions of the equations

$$Sx = S(Ax - BH^\pm x - BE^\pm) = 0,$$

with non-degeneracy conditions

$$SJ^\pm f^\pm \neq 0 \quad \text{and} \quad \det(SJ^+, SJ^-, S) \neq 0$$

and we have  $w^\pm = \pm(SJ^\mp f^\pm)/(\sqrt{-SJ^+ f^+ - SJ^- f^-})$ .

**Example.** The following MIMO control model was shown by Colombo et al. (2010) to exhibit invisible canards. Consider (20) with  $S = (1 \ 0)$ , and

$$A = \begin{pmatrix} -1 & 1 & 0 \\ -1 & 0 & 1 \\ -1 & 0 & 0 \end{pmatrix}, \quad B = \begin{pmatrix} 1 & 0 \\ 0 & 1 \\ \mu & 0 \end{pmatrix}, \quad C = \begin{pmatrix} 1 & 0 & 0 \\ 0 & 0 & 1 \end{pmatrix},$$

$$H^\pm = \begin{pmatrix} 0 & \mp 1 \\ 0 & 0 \end{pmatrix}, \quad E^+ = \begin{pmatrix} 1 \\ 2 \end{pmatrix}, \quad E^- = \begin{pmatrix} -2 \\ -4 \end{pmatrix},$$

for  $\mu \in \mathbb{R}$ . The switching manifold is the surface  $x_1 = 0$ , and the two-fold is the point  $x = (0, -1/2, 3/2)^\top$ . At the two-fold,  $f^+ = (0, -1/2, \mu/2)^\top$  and  $f^- = (0, 11/2, \mu/2)^\top$ , which are antiparallel when  $\mu = 0$ , for which  $w^+ w^- = 1$  and  $w^\pm < 0$ . In Fig. 8 we simulate the system for  $\mu = 0.01$

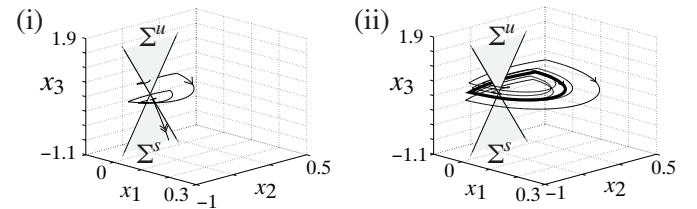


Fig. 8. Orbits of the MIMO system for: (i)  $w^+ w^- = 1.02$ , and (ii)  $w^+ w^- = 0.64$ . A typical orbit is shown winding around the two-fold. In (i) the orbit starts in  $\Sigma^u$  and lands in  $\Sigma^s$ , then slides away from the two-fold. In (ii) the orbit is attracted to a stable periodic orbit (bold). Simulation from Colombo et al. (2010).

and  $\mu = -0.2$ , corresponding to  $w^+ w^- = 1.022$  and  $w^+ w^- = 0.64$  respectively, both cases involving faux canards. The figure shows that for  $w^+ w^- > 1$  orbits reach the sliding region after crossing the switching manifold a finite number of times, while for  $w^+ w^- < 1$  orbits are attracted to a stable periodic orbit encircling the two-fold, forming a controllable oscillatory mode dependent upon  $\mu$ . As  $\mu \rightarrow 0$  the periodic orbit shrinks toward the two-fold and disappears.

#### 4.3 A linear system with non-deterministic chaos

The following piecewise linear system was introduced by Colombo and Jeffrey (2011) as an example of the non-deterministic form of chaos described in section 3.4. Here we recast the system in terms of the control model (20), though not in observable canonical form. The switching function is again taken as  $\sigma(x) = x_1$ , and we consider a system with three inputs and three outputs, letting

$$A = \frac{1}{2} \begin{pmatrix} 0 & -1 & 1 \\ -1 & -5 & 0 \\ 1 & 1 & 1 \end{pmatrix}, \quad B = \frac{1}{2} \begin{pmatrix} 6 & 1 & 1 \\ 1 & 1 & 0 \\ 1 & -1 & 5 \end{pmatrix},$$

with  $S = (1, 0, 0)$ ,  $H = \pm C$ , where  $C$  is the  $3 \times 3$  identity matrix as for full state feedback, and we let

$$E^+ = -B^{-1} \begin{pmatrix} 0 \\ 1 \\ w^+ \end{pmatrix}, \quad E^- = -B^{-1} \begin{pmatrix} 0 \\ w^- \\ 1 \end{pmatrix},$$

where  $w^\pm$  are real constants corresponding to those in (12). Then there is a two-fold at the origin, which is of invisible type by (17a) since a simple calculation shows  $\mathcal{L}_{f^\pm}^2 \sigma = \mp 1$ . To observe a canard we must then choose  $w^\pm < 0$  such that  $w^+ w^- > 1$  by (17b). Figs. 9 and 10 show the simulation of a typical orbit in the system

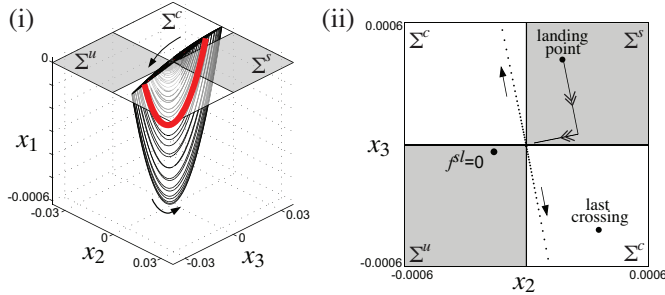


Fig. 9. Simulation of a typical orbit in a non-deterministic chaotic system with  $w^+ = -5.01$  and  $w^- = -1/5$ . The sliding regions  $\Sigma^s$  (stable) and  $\Sigma^u$  (unstable) are shaded. (i) The orbit winds around the two-fold at the origin, and around an unstable periodic orbit (bold) passing through the crossing regions  $\Sigma^c$  (unshaded). (ii) Magnification in the plane of  $\Sigma$ , showing crossing points (dots) of an orbit which leaves the neighbourhood of the two-fold, then returns and lands in  $\Sigma^s$ , followed by sliding towards the two-fold. A zero of  $f^{sl}$  can be seen in  $\Sigma^u$ . Simulation from Colombo and Jeffrey (2011).

with  $w^+ = -5.01$  and  $w^- = -1/5$ , from an initial point  $x = (10^{-20}, -10^{-6}, -10^{-6})$ , which lies above the unstable sliding region a small distance from the two-fold. We have then  $w^+ w^- = 1.002$ , meaning the vector fields  $f^\pm$  are almost antiparallel at the two-fold, causing a crossing orbit to be almost planar as it winds around the two-fold, as seen in Fig. 9. In Fig. 10 the same orbit is shown after a linear coordinate change in the  $x_2$ - $x_3$  plane to unflatten the orbit, and a stretch of the coordinate  $x_1$  by a factor 20 for  $x_1 > 0$  only, to resolve its trajectory above the switching manifold.

In Fig. 9(ii) the region of  $\Sigma$  in the neighbourhood of the two-fold is magnified, showing the locus of points where the simulated orbit crosses  $\Sigma$ , or equivalently, showing the return map from each region  $\Sigma^c$  to itself. After the last crossing (lower right corner), the orbit enters the stable sliding region and slides for a time  $t \simeq 0.48$  before reaching the two-fold. At this time numerical integration fails because  $f^{sl}$  becomes set-valued. Repeated simulations with different (local) initial conditions confirm that all orbits behave similarly, returning to the two-fold in finite time after excursions of widely varying times and distances.

## 5. CONCLUDING REMARKS

While these examples demonstrate the classification of two-fold singularities and their dynamics, explicit physical models exhibiting explosions due to non-determinism are the subject of ongoing study. By unraveling the dynamics of these phenomena we seek to raise the question of what forms of control system they can occur in, either by

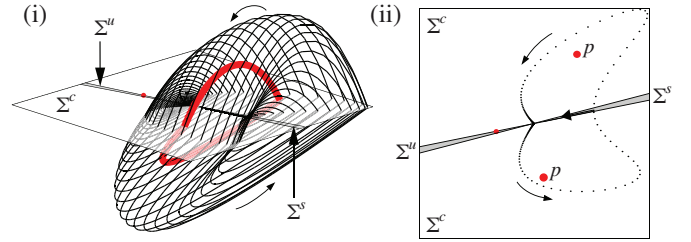


Fig. 10. Scaled image resolving the orbit from Fig. 9. (i) The orbit winds around the two-fold and the periodic orbit. (ii) The locus of crossing points of the orbit, surrounding the periodic orbit (labeled  $p$ ). The zero of  $f^{sl}$  in  $\Sigma^u$  and the orbit's attraction to the two-fold inside  $\Sigma^s$  are also shown. Compare this simulation, originally from Colombo and Jeffrey (2011), to Fig. 7.

accident or by design. As noted at the end of section 3.1, an experimental control device exhibiting a grazing explosion is known, where the effect is due to sudden jumps between normal and superconducting modes of a resonator.

As suggested in section 3.3, some discontinuity induced phenomena can be associated with canard-like behaviour in singularly perturbed systems, suggesting the term *explosions* for the loss of determinacy they create. They provide both isolated events and robust situations in which orbits can have counterintuitive evolution, *from* strongly attracting regions of phase space, *to* strongly repelling regions. Such counterintuitive phenomena can arise in stiff nonlinear or, as we show here, discontinuous, systems.

## REFERENCES

- Benoît, E., Callot, J.L., Diener, F., and Diener, M. (1981). Chasse au canard. *Collect. Math.*, 31-32, 37-119.
- Colombo, A., di Bernardo, M., Fossas, E., and Jeffrey, M.R. (2010). Teixeira singularities in 3D switched feedback control systems. *Systems & Control Letters*, 59(10), 615-622.
- Colombo, A. and Jeffrey, M.R. (2011). Non-deterministic chaos, and the two-fold singularity in piecewise smooth flows. *SIAM J. App. Dyn. Sys.* (accepted).
- Desroches, M. and Jeffrey, M.R. (2011). Canards and curvature: nonsmooth approximation by pinching. *Non-linearity* (accepted).
- di Bernardo, M., Budd, C.J., Champneys, A.R., and Kowalczyk, P. (2008). *Piecewise-Smooth Dynamical Systems: Theory and Applications*. Springer.
- di Bernardo, M., Kowalczyk, P., and Nordmark, A. (2003). Sliding bifurcations: a novel mechanism for the sudden onset of chaos in dry friction oscillators. *Int. J. Bif. Chaos*, 10, 2935-2948.
- Filippov, A.F. (1988). *Differential Equations with Discontinuous Righthand Sides*. Kluwer Academic Publ. Dordrecht.
- Jeffrey, M.R., Champneys, A.R., di Bernardo, M., and Shaw, S.W. (2010). Catastrophic sliding bifurcations and onset of oscillations in a superconducting resonator. *Phys. Rev. E*, 81(1), 016213-22.
- Jeffrey, M.R. and Hogan, S.J. (2011). The geometry of generic sliding bifurcations. *SIAM Review* (accepted).
- Kuznetsov, Y.A. (1998). *Elements of Applied Bifurcation Theory*. Springer, 2nd Ed.
- Utkin, V.I. (1977). Variable structure systems with sliding modes. *IEEE Trans. Automat. Contr.*, 22.